

# Perspectives on the Formation of Peakons in the Stochastic Camassa-Holm Equation

Thomas M. Bendall<sup>1</sup>, Colin J. Cotter<sup>1</sup>, and Darryl D. Holm<sup>1</sup>

<sup>1</sup>*Mathematics Department, Imperial College London, UK*

April 12, 2022

## Abstract

The stochastic Camassa-Holm equation was derived in Holm and Tyranowski (2016) from the stochastic variational formulation of Holm (2015). Holm and Tyranowski (2016) also derived stochastic differential equations describing the evolution of the momenta and positions of peakon solutions. The work of Crisan and Holm (2018) then showed that in the stochastic Camassa-Holm equation peakons form with positive probabilities. This probability has not however yet been shown to be unity, unlike the deterministic case. We attempt to extend this discussion, by showing that peakons satisfying the stochastic differential equations presented in Holm and Tyranowski (2016) do indeed satisfy the stochastic Camassa-Holm equation, by writing the stochastic Camassa-Holm equation in a hydrodynamic form. Then we present a finite element discretisation of the stochastic Camassa-Holm equation, which we show numerically converges to the stochastic differential equations governing the evolution of peakons. We proceed to use this discretisation to numerically investigate the probability of peakons forming in the stochastic Camassa-Holm equation.

## 1 Introduction

### 1.1 Overview

We are dealing with robustness of singular solution behaviour for continuum PDEs under stochastic perturbations. This is a well-known subject for SPDEs in fluid dynamics which form shocks by producing a vertical derivative in their solution profile in finite time. This is also known as *wave breaking*. For example, a well-studied topic in this field is the robustness of shock formation by the 1D Burgers equation ( $u_t + 3uu_x = 0$ ) by the following stochastic perturbation

$$du(x, t) + (\partial_x u + u\partial_x)(u dt + \Xi(x) \circ dW_t) = 0, \quad (1.1)$$

for the evolution in time  $t \in \mathbb{R}$  of fluid momentum density  $u(x, t)$  on the real line  $x \in \mathbb{R}$  under stochastic perturbations [1]. In equation (1.1), the time differential  $d$  is short notation for a stochastic integral; the spatial partial derivative  $\partial_x$  acts rightward on all products; the symbol  $\circ$  denotes a Stratonovich stochastic process;  $dW_t$  is a Brownian motion with spatially modulated amplitude  $\Xi(x)$ ; and one interprets the effect of the stochasticity as a noisy perturbation of the transport velocity. See [1] for more discussion.

Such stochastic perturbations are of current interest in the modelling of geophysical fluids, where

they can express the uncertainty in the effects of the unresolved processes upon the resolved flow. In this context, a new class of stochastic fluid equations was introduced by [2], which crucially preserve many of the circulation properties of the respective deterministic equations. For instance in the stochastic quasi-geostrophic equations studied by [3] and [4], the potential vorticity is still preserved by material transport. These equations are derived from a stochastically constrained variational principle  $\delta S = 0$ , where the action  $S$  is given by

$$S = (\mathbf{u}, p, q) = \int [\ell(\mathbf{v}, q) dt + \langle p, dq + \mathfrak{L}_{d\mathbf{x}_t} q \rangle], \quad (1.2)$$

where  $\mathbf{u}$  is the velocity advecting quantity  $q$  and  $\ell(\mathbf{u}, q)$  is the Lagrangian of the deterministic fluid. The Lagrange multiplier  $p$  enforces the stochastic transport of  $q$  by the Lie derivative  $\mathfrak{L}_{d\mathbf{x}_t}$  along a vector field  $d\mathbf{x}_t$ , which is given by

$$d\mathbf{x}_t = \mathbf{u}(\mathbf{x}, t) dt - \sum_j \Xi^j(\mathbf{x}) \circ dW^j(t), \quad (1.3)$$

with the sum over multiple Wiener processes. The angled brackets denote the spatial integral over the domain  $\Omega$  of the pairing of  $p$  and  $q$ ,

$$\langle p, q \rangle = \int_{\Omega} pq dx. \quad (1.4)$$

A thorough description of this formulation can be found in [2].

The following PDE is known as the Camassa–Holm (CH) equation [5],

$$m_t(x, t) + (\partial_x m + m \partial_x) u = 0, \quad \text{with} \quad m = u - \alpha^2 u_{xx}. \quad (1.5)$$

The CH equation (1.5) was derived at one order beyond the celebrated Korteweg-de Vries (KdV) equation in the asymptotic expansion of the Euler fluid equations for non-linear shallow water waves on a free surface propagating under the restoring force of gravity. Unlike the Burgers equation in (1.1), evolution by the CH equation (1.5) does not create shocks. Instead, CH creates a type of singular solution known as a *peakon* which possesses a sharp peak at the apex of its velocity profile.

The formation of the sharp peak in the singular peakon solution does not occur by wave breaking and the creation of a vertical slope in the velocity profile. Instead, numerical simulations reveal that peakons arise an intriguing process in which a pair of inflection points of opposite slope are created during the evolution of a spatially confined smooth initial profile. Then the two leading inflection points rise together as the height of the velocity between them increases and thereby the flow leaves the remainder of the profile behind,. The two leading inflection points continue to rise until they collide to create the peakon’s sharp peak.

The shape of the peakon profile turns out to be the Green’s function for the Helmholtz operator which relates the velocity  $u$  and the momentum density  $m$  in equation (1.5). This shape may be explained by recalling that the peakon solutions for the momentum density in (1.5) may be expressed by the singular momentum map [6],

$$m(x, t) = \sum_{a=1}^N p_a(t) \delta(x - q_a(t)) \quad \text{so} \quad u(x, t) = \sum_{a=1}^N p_a(t) K(x - q_a(t)), \quad (1.6)$$

in which  $K(x - q_a(t)) = \frac{1}{2} \exp(-|x - q_a(t)|/\alpha)$  is the Green's function for the Helmholtz operator on the real line with homogeneous boundary conditions. Remarkably, the purely discrete spectrum of the isospectral eigenvalue equation which demonstrates that the CH equation is a completely integrable Hamiltonian soliton system also implies that *only* the singular solutions in (1.6) will persist.

The aim of this paper is to study robustness of peakon formation by the stochastic Camassa-Holm (SCH) equation under the following stochastic perturbation,

$$dm(x, t) + (\partial m + m\partial)(u dt + \sum_j \Xi^j(x) \circ dW^j) = 0, \quad \text{with } m = u - \alpha^2 u_{xx}. \quad (1.7)$$

See [2, 7] for more discussion of the derivation and analysis of the SCH equation in (1.7) and see [8] for discussions of its solution behaviour and the development of computational algorithms for numerical simulations of its solution behaviour.

While the introduction of stochastic transport into SCH cannot be expected to preserve the complete integrability of the unperturbed CH equation, one may ask whether the initial value problem for SCH still produces peakons on the real line. The present paper answers that question affirmatively via numerical simulation.

In this paper, we extend the work of [8], who originally derived the stochastic Camassa-Holm equation (1.17) in the EPDiff regime. The authors then presented a discretisation of the stochastic ordinary differential equations describing the evolution of peakons, and used this discretisation to explore the interaction of peakons. The other main work which we develop is that of [7], who showed the probability of peakon formation in this regime is positive, though not necessarily unity. This can be compared with the deterministic case, in which peakons always form from an inflection point upon a negative slope within finite time. We attempt to extend this by investigating peakon formation numerically.

Here is the paper's structure. In Section 2, we verify that peakons do indeed satisfy the stochastic Camassa-Holm equation via writing it in hydrodynamic form. In Section 3 we present a finite element discretisation for the stochastic Camassa-Holm equation in the EPDiff regime, showing its numerical convergence properties in Section 4. In Section 5, we numerically investigate the steepening lemma of [7] using our discretisation.

## 1.2 Forms of the Deterministic Camassa-Holm Equation

In this paper, we will build on the work of [8] and [7] in exploring the properties of the Camassa-Holm equation within this stochastic framework. The Camassa-Holm equation was introduced in [5], and describes one-dimensional dispersive shallow-water waves. It has a bi-Hamiltonian structure and possesses special soliton solutions, which propagate at constant velocity without changing shape or amplitude, as non-linear and dispersive effects cancel out. Here we briefly present the deterministic equation in three different forms.

The first form of the equation, for velocity  $u$  and parameter  $\alpha$  is

$$u_t - \alpha^2 u_{xxt} + 3uu_x = 2\alpha^2 u_x u_{xx} + \alpha^2 uu_{xxx}, \quad (1.8)$$

with subscripts  $x$  and  $t$  denoting partial derivatives with respect to spatial coordinate  $x$  and time  $t$  respectively.

The Hamiltonian structure of (1.8) is commonly exploited to write it as the coupled equations

$$m = u - \alpha^2 u_{xx}, \quad (1.9a)$$

$$m_t + (mu)_x + mu_x = 0, \quad (1.9b)$$

where  $m$  can be treated as a momentum that is related to  $u$  via a Helmholtz operator.

A third form of (1.8), which we call the hydrodynamic form, can be derived by first writing (1.9b) as an operation upon  $m$ , which combined with the definition of  $m$  gives the following equation for  $u$ :

$$(\partial_t + \partial_x u + u_x) (1 - \alpha^2 \partial_x^2) u = 0. \quad (1.10)$$

The left hand side describes the action of two operators, and we find the result of alternating their order by introducing the commutator, so that

$$(1 - \alpha^2 \partial_x^2) (\partial_t + \partial_x u + u_x) u = - [\partial_t + \partial_x u + u_x, 1 - \alpha^2 \partial_x^2] u. \quad (1.11)$$

Inspection of the commutator shows that it can be written as the gradient of a potential. Applying the inverse Helmholtz operator to both sides, which commutes through the gradient, gives

$$(\partial_t + \partial_x u + u_x) u = -\partial_x K * \left[ \alpha^2 (u^2)_{xx} + \frac{\alpha^2}{2} (u_x)^2 \right] \quad (1.12)$$

Noticing that the non-linear term on the left can also be written as a gradient, and using  $K * (u - \alpha^2 u_{xx}) = u$ , gives the final hydrodynamic form of the Camassa-Holm equation,

$$u_t = -\partial_x \left\{ \frac{1}{2} u^2 + K * \left[ u^2 + \frac{\alpha^2}{2} (u_x)^2 \right] \right\}. \quad (1.13)$$

The significance of this form of the equation is that no second derivative of  $u$  directly appears in the equation. Further, this equation admits weak peakon solutions, as will be discussed in Section 2.

Equations (1.8), (1.9) and (1.13) are equivalent ways of expressing the Camassa-Holm equation.

### 1.3 The Stochastic Camassa-Holm Equation

The deterministic equation (1.9) can be found by exploiting the Hamiltonian structure:

$$m_t = -(\partial_x m + m \partial_x) \frac{\delta H}{\delta m}, \quad (1.14)$$

with the Hamiltonian

$$H = \frac{1}{2} \int_{\Omega} (u^2 + \alpha^2 u_x^2) dx = \frac{1}{2} \int_{\Omega} m (K * m) dx, \quad (1.15)$$

in which case  $\delta H / \delta m = u$ . A similar approach can be used to find the stochastic Camassa-Holm equation, as used in [7]. In this case, we introduce the stochastic Hamiltonian

$$d\mathcal{H} = \frac{1}{2} \int_{\Omega} m (K * m) dt dx + \int_{\Omega} m \sum_j \Xi^j \circ dW^j dx. \quad (1.16)$$

The respective variational derivative is then  $\delta d\mathcal{H}/\delta m = dx_t$ , with  $dx_t$  from (1.3). The resulting stochastic equation is then

$$dm = -(m dx_t)_x - m (dx_t)_x, \quad (1.17)$$

which can be thought of as the stochastic case of (1.9). This equation also possesses a hydrodynamic form, which can also be obtained by considering the commutator

$$[d + \partial_x dx_t + \partial_x (dx_t), 1 - \alpha^2 \partial_x^2] u = \alpha^2 [2u_{xx} (dx_t)_x + 5u_x (dx_t)_{xx} + 2u (dx_t)_{xxx}]. \quad (1.18)$$

Separating this into deterministic and stochastic parts gives

$$\begin{aligned} (d + \partial_x dx_t + (dx_t)_x) u &= -K * [\alpha^2 (7u_x u_{xx} + 2uu_{xx})] dt \\ &\quad - \sum_j K * [\alpha^2 (2u_{xx} \Xi_x^j + 5u_x \Xi_{xx}^j + 2u \Xi_{xxx}^j)] \circ dW^j, \end{aligned} \quad (1.19)$$

which results in

$$\begin{aligned} du &= -\partial_x \left\{ \frac{1}{2} u^2 + K * \left[ u^2 + \frac{\alpha^2}{2} (u_x)^2 \right] \right\} dt \\ &\quad - \sum_j \left\{ u_x \Xi^j + K * [2u \Xi_x^j + \alpha^2 u_x \Xi_{xx}^j] \right\} \circ dW^j. \end{aligned} \quad (1.20)$$

Unlike (1.13), the right hand side of (1.20) cannot be written purely as a gradient, but it also contains no double derivatives of  $u$ .

## 2 Peakon Solutions to the Stochastic Camassa-Holm equation

In the hydrodynamic form (1.20), the equation admits weak peakon solutions, of the form

$$u = K * [\delta(x - q(t)) p(t)] = p(t) e^{-|x - q(t)|/\alpha}, \quad (2.1)$$

in which  $q(t)$  represents the position of the peakon and  $p(t)$  represents its momentum, and together they form a pair of canonical coordinates satisfying a Hamiltonian system. As stated in [7], the Hamiltonian of this stochastic system of  $M$  peakons can be written as

$$dh = \frac{1}{4} \sum_{a,b=1}^M p_a(t) p_b(t) e^{-|q_a(t) - q_b(t)|/\alpha} \quad (2.2)$$

The evolution of these canonical coordinates is described by the pair of coupled stochastic differential equations

$$dp_a = -\frac{\partial dh}{\partial q_a} = -p_a(t) \frac{\partial dx_t(q_a(t))}{\partial q}, \quad (2.3a)$$

$$dq_a = \frac{\partial dh}{\partial p_a} = dx_t(q_a(t)), \quad (2.3b)$$

where

$$dx_t(q_a(t)) = u(q_a(t)) dt + \sum_j \Xi^j(q_a(t)) \circ dW^j. \quad (2.4)$$

Considering a single peakon and writing  $u = p(t) \exp(-|x - q(t)|/\alpha)$ , gives

$$dx_t(q(t)) = p(t) dt + \sum_j \Xi^j(q(t)) \circ dW^j. \quad (2.5)$$

In [7] it was argued that substitution of (2.3) into (2.1) yields (1.17). However, the peakon solution (2.1) only makes sense as a weak solution to (1.20), the verification of which is the focus of this section. In other words, they are solutions to

$$\begin{aligned} \int_{\Omega} \phi du dx &= \int_{\Omega} \phi_x \left\{ \frac{1}{2} u^2 + K * \left[ u^2 + \frac{\alpha^2}{2} (u_x)^2 \right] \right\} dt dx \\ &\quad - \sum_j \int_{\Omega} \phi \left\{ u_x \Xi^j + K * [2u \Xi_x^j + \alpha^2 u_x \Xi_{xx}^j] \right\} dx \circ dW^j, \end{aligned} \quad (2.6)$$

for all  $\phi \in H^1$ .

To verify that such peakons do indeed satisfy this equation, we take  $\phi = A \cos(kx) + B \sin(kx)$  and  $\Xi^j = C_j \cos(jx) + D_j \sin(jx)$ . Using (2.1) and (2.3), we write the differential  $du$  as

$$du = \frac{u}{p} dp - \frac{u}{\alpha} \text{sign}(x - q) dq, \quad (2.7)$$

$$= -\frac{pu}{\alpha} \text{sign}(x - q) dt - u \sum_j \left[ \frac{1}{\alpha} \Xi^j(q) \text{sign}(x - q) + \Xi_x^j(q) \right] \circ dW^j. \quad (2.8)$$

The  $K*$  operation is performed upon some  $f(x)$  as

$$K * f = \int_{\Omega} e^{-|x-y|/\alpha} f(y) dy. \quad (2.9)$$

Taking the domain  $\Omega$  as  $\mathbb{R}$  and combining these elements to compute the integrals, both right and left hand sides of (2.6) return

$$\begin{aligned} &\frac{2p^2 \alpha k}{1 + \alpha^2 k^2} [B \cos(kq) - A \sin(kq)] dt \\ &\quad - \frac{2p\alpha}{1 + \alpha^2 k^2} \sum_j [(BC_j k - AD_j j) \cos(jq) \cos(kq) - (AC_j k + BD_j j) \cos(jq) \sin(kq) \\ &\quad \quad + (AC_j j + BD_j k) \sin(jq) \cos(kq) + (BC_j j - AD_j k) \sin(jq) \sin(kq)] \circ dW^j, \end{aligned} \quad (2.10)$$

thus verifying that  $u = p(t) \exp[-|x - q(t)|/\alpha]$  is a solution to (2.6), if  $p$  and  $q$  satisfy (2.3).

### 3 A Finite Element Discretisation for the Stochastic Camassa-Holm Equation

Here we present a mixed finite element discretisation of the stochastic Camassa-Holm equation, inspired by the form (1.20), to have confidence in the discrete representation of peakons.

Considering the space  $V$  of continuous linear functions, we seek to find the

$$\left( u^{(n+1)}, \Delta F^{(h)}, \Delta G^{(h)} \right) \in (V, V, V) \quad (3.1)$$

that satisfy, for all  $(\psi, \phi, \zeta) \in (V, V, V)$ , the equations

$$\int_{\Omega} \psi \left( u^{(n+1)} - u^{(n)} \right) dx + \int_{\Omega} \psi u_x^{(h)} \Delta v^{(h)} dx - \int_{\Omega} \psi_x \Delta F^{(h)} dx + \int_{\Omega} \psi \Delta G^{(h)} dx = 0, \quad (3.2a)$$

$$\int_{\Omega} \phi \Delta F^{(h)} dx + \alpha^2 \int_{\Omega} \phi_x \Delta F_x^{(h)} dx - \int_{\Omega} \phi u^{(h)} u_x^{(h)} \Delta t dx - \frac{\alpha^2}{2} \int_{\Omega} u_x^{(h)} u_x^{(h)} \Delta t dx = 0, \quad (3.2b)$$

$$\int_{\Omega} \zeta \Delta G^{(h)} dx + \alpha^2 \int_{\Omega} \zeta_x \Delta G_x^{(h)} dx - \sum_j \left( \int_{\Omega} 2\zeta u^{(h)} \Xi_x^j - \alpha^2 u^{(h)} \Xi_{xx}^j \right) \Delta W^j dx = 0, \quad (3.2c)$$

where  $\Delta t$  is the time step,  $u^{(n)}$  is the value of  $u$  at the  $n$ -th time level, and we have used the implicit midpoint rule to discretise in time, so that  $u^{(h)} = \frac{1}{2}(u^{(n+1)} + u^{(n)})$ . The stochastic velocity  $\Delta v^{(n+1/2)}$  is given by

$$\Delta v^{(n+1/2)} = u^{(n+1/2)} \Delta t + \sum_j \Xi^j \Delta W^j, \quad (3.3)$$

and  $\Delta W^j$  is a normally distributed number with zero mean and variance  $\Delta t$ .

## 4 Convergence of the Discretisation to Peakon Solutions

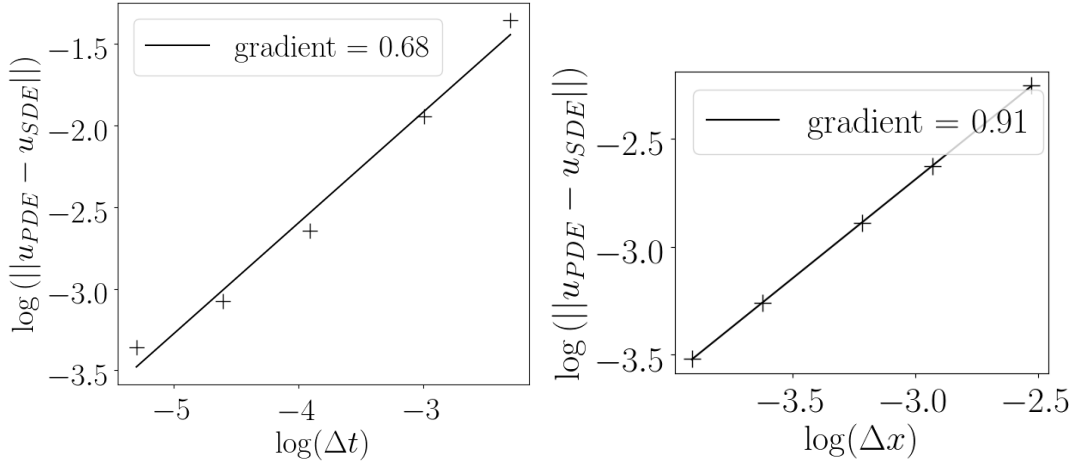


Figure 1: (Left) a plot showing the strong convergence of the numerical discretisation with  $\Delta t$ . This plot thus shows that as  $\Delta t \rightarrow 0$ , the solution converges for individual realisations of the noise. (Right) a plot showing the convergence as  $\Delta x \rightarrow 0$  of the discretisation from Section 3 of the stochastic Camassa-Holm equation to the equations (4.1) describing the evolution of peakon solutions. For both plots, the true solution was computed by solving (4.1), and using this to create the  $u$  field corresponding to a peakon solution of momentum  $p$  and position  $q$  within the discretisation from Section 3. Crosses mark the data points, with a solid best fit line overlaid.

In this section, we show that when describing the evolution of a peakon, our discretisation

presented in Section 3 converges to the equations

$$dp = \frac{p}{2} \sum_j \left[ (\Xi_x^j(q))^2 - \Xi^j(q) \Xi_{xx}^j(q) \right] dt - p \sum_j \Xi_x^j(q) dW^j, \quad (4.1a)$$

$$dq = \left[ p + \frac{1}{2} \sum_j \Xi^j(q) \Xi_x^j(q) \right] dt + \sum_j \Xi^j(q) dW_j. \quad (4.1b)$$

To do this, we set up a periodic one-dimensional domain of length  $L_d = 40$ , and taking  $\alpha = 1$ , we specify an initial condition of

$$u = \begin{cases} \exp[(x - L_d/2)/\alpha], & x < L_d/2, \\ \exp[-(x - L_d/2)/\alpha], & x \geq L_d/2. \end{cases} \quad (4.2)$$

First we establish a numerical solution of (4.1) that is well-resolved temporally, by solving (4.1) using a simple forward Euler timestepping scheme, with initial condition of  $p = 1$  and  $q = 20$  and with  $\Delta t = 10^{-5}$ . For the stochastic basis functions, we used only a single function:

$$\Xi^0 = 0.02 \sin\left(\frac{4\pi x}{L_d}\right). \quad (4.3)$$

Then we performed two tests, one showing the strong convergence of the discretisation (3.2) to this high resolution solution of (4.1) as  $\Delta t$  approached  $10^{-5}$ . This was performed at fixed spatial resolution with  $\Delta x = 40/2000$ . The second test showed convergence of (3.2) to (4.1) as  $\Delta x \rightarrow 0$ , using  $\Delta t = 10^{-5}$ .

When solving our discretisation (3.2) with a larger time step, say  $n\Delta t$ , to ensure that the realisation of the noise corresponded to those with  $\Delta t$ , the random number used for that larger time step would be  $\frac{1}{\sqrt{n}} \sum_i^n \Delta W$ , where  $\Delta W$  are the random numbers corresponding to the smaller  $\Delta t$ . At a given time step, the  $p$  and  $q$  calculated from (4.1) were translated into the  $u$  field corresponding to a peakon in the discretisation of the PDE using (2.1), which could be compared with the  $u$  found from solving (3.2).

Results showing the strong temporal convergence of the discretisation are shown in Figure 1 (left), whilst Figure 1 (right) displays the results of the spatial convergence of the discretisation to the underlying stochastic differential equations for the evolution of the peakon.

## 5 Numerical Investigations of the Steepening Lemma

One of the key results of [7] was the investigation of the steepening lemma for the stochastic Camassa-Holm system. In the deterministic case, a peakon will always form in finite time from an inflection point on a negative slope, which was one of the key results of [5]. In [7], it was shown that there was a non-zero probability of a peakon forming in these conditions in the stochastic Camassa-Holm system. In this section we attempt to investigate, numerically, whether this probability is simply non-zero or almost unity.

To add to this discussion, we perform numerical simulations of the stochastic Camassa-Holm equation, using the discretisation of Section (3), under many different realisations of the noise, and record the formation of peakon solutions. The first step in this investigation is to determine a numerical diagnostic for whether a solution is in fact a peakon. Our diagnostic used is the



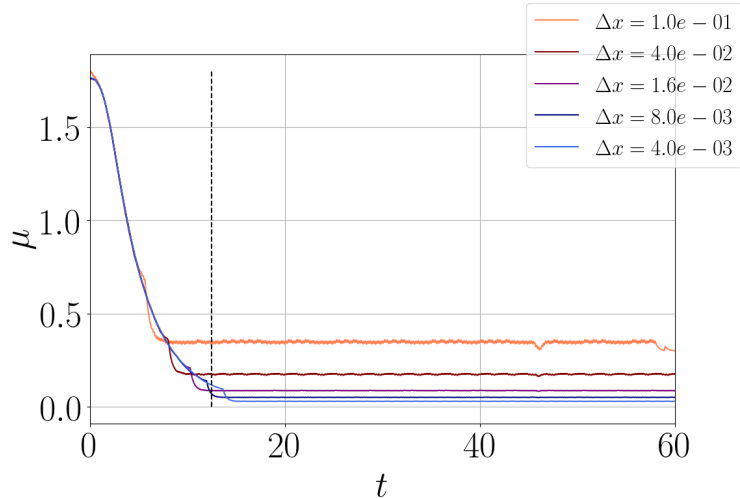


Figure 2: The evolution of  $\mu$ , the distance between inflection points, for the deterministic case with initial condition given by (5.1). This is plotted at various resolutions, illustrating that initially, in the absence of a peakon,  $\mu$  converges to a non-zero number. As the peakon forms, this measure is no longer converged, and as  $\Delta x \rightarrow 0$ ,  $\mu \rightarrow 0$ . Due to errors in measuring the location of the inflection points within a cell,  $\mu$  can be very noisy. To reduce this, we applied a low pass filter to  $\mu$ . An interesting feature of the evolution of  $\mu$  is a fairly sudden drop in the values at around  $t = 10$ .

distance between inflection points in  $u$  in the discretisation, which we denote as  $\mu$ . For a smooth peak, as  $\Delta x \rightarrow 0$ ,  $\mu$  will converge to some non-zero value, whilst for a peaked solution,  $\mu$  will converge to zero as  $\Delta x \rightarrow 0$ .

As a peakon forms, values of  $\mu$  calculated at different resolutions diverge, as illustrated in Figure 2, which shows the evolution of a peakon within the discretisation of Section 3 at differing resolutions. This figure was produced in a domain of length  $L_d = 40$ , with a time step of  $\Delta t = 0.001$ , and with the initial condition set as

$$u = \frac{1}{\exp(x - x_c) + \exp(x_c - x)}, \quad (5.1)$$

with  $x_c = 203/15$ . We have applied a low-pass filter to the  $\mu$  values so as to reduce error in the measurement of the positions of the inflection points. This data can be used to approximate a time for the formation of the peakon, which we take to be the time at which the gradient of the best fit line of  $\log(\mu)$  as a function of  $\log(\Delta x)$  at a given time breaches a certain threshold, which we take to be 0.4.

Extending this approach to stochastic simulations, again using the initial condition (5.1), the histograms showing the evolution of  $\mu$  over many different realisations (as a function of time  $t$  and resolution  $\Delta x$ ) are shown in Figure 3. This experiment was performed for 1000 realisations of the noise, where the stochastic basis functions were  $n = 1, 2, \dots, 6$  of

$$\Xi^n = \begin{cases} 0.08 \sin((n+1)\pi x/L_d), & n \text{ is odd,} \\ 0.08 \cos(n\pi x/L_d), & n \text{ is even} \end{cases} \quad (5.2)$$

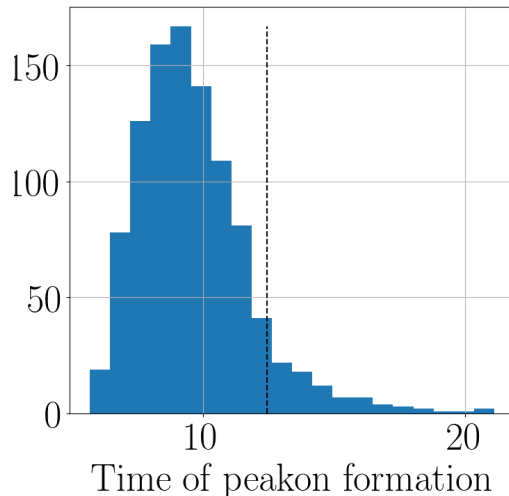


Figure 3: A histogram showing the estimated time of peakon formation for 1000 realisations of the noise (5.2) from the initial state (5.1). The dashed black line shows the peakon formation time from the deterministic case. These times are determined to be the first time at which the gradient of the linear best fit curve of  $\log(\mu)$  against  $\log(\Delta x)$ , at a given time, exceeded a threshold, which we chose to be 0.4. The implication of this plot is that the effect of the noise upon peakon formation is to make it occur earlier.

Figure 4 clearly shows that the inflection points move closer together as both time evolves, and  $\Delta x \rightarrow 0$ . The histogram showing the peakon formation times from these realisations of the noise is shown in Figure 3.

In all these realisations of the noise, a peakon was adjudged to have formed, providing supporting evidence for the hypothesis that peakons form with a probability of unity in the stochastic Camassa-Holm equation from a smooth initial condition with an inflection point on a negative slope, which is clearly not something that can be explicitly proved experimentally. In fact, the evidence from Figures 3 and 4 is that the stochastic noise prompts the peakon solution to emerge more quickly in the deterministic case.

## 6 Conclusions

We have extended the discussion of peakons within the stochastic Camassa-Holm equation begun by [8] and [7]. This first result was a demonstration that peakons satisfying the equations (2.3) derived in [8] do indeed satisfy the stochastic Camassa-Holm equation (1.20) when it is cast in hydrodynamic form. Next, we presented a new finite element discretisation for (1.20). We then showed numerically that this discretisation converges both strongly in time and also converges to (4.1) as  $\Delta x \rightarrow 0$ . This discretisation then provided a tool with which to investigate the steepening lemma of [7] for the stochastic Camassa-Holm system. Starting with smooth initial conditions, we investigated the formation of peakons under different realisations of the stochastic noise. No examples without peakon formation were found, and the noise was observed to tend to lead to faster peakon formation.

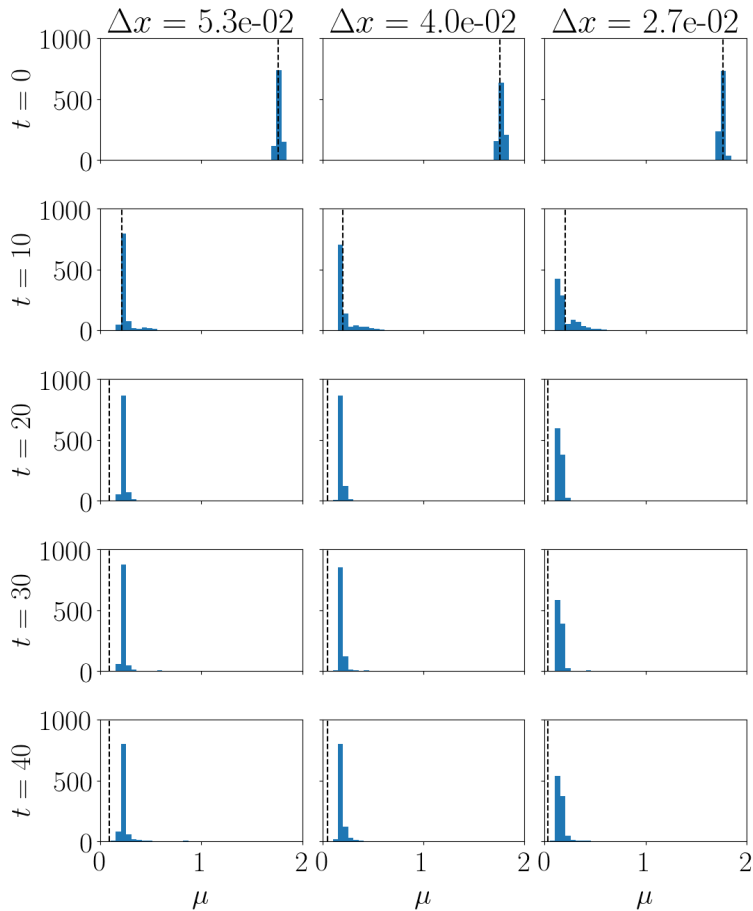


Figure 4: Histograms of  $\mu$ , the distance between inflection points of the profile, over many realisations of the noise. The experiments were all initialised with the condition (5.1), and plotted here are the evolutions of  $\mu$  with time at different resolutions  $\Delta x$  of the discretisation. In each panel, the dashed black line shows the value of  $\mu$  in the deterministic case at that resolution. These plots illustrate that  $\mu$  becomes much smaller as the peakon solution forms from the smooth initial condition. It also shows that as  $\Delta x \rightarrow 0$ , before the peakon forms,  $\mu$  converges to some non-zero number, but once the peakon has formed it converges to zero. It is also interesting to note that the  $\mu$  measured in the deterministic case tends to be smaller than in the stochastic cases.

## Acknowledgements

TMB was supported by the EPSRC Mathematics of Planet Earth Centre for Doctoral Training at Imperial College London and the University of Reading, with grant number EP/L016613/1. TMB and CJC were also supported by EPSRC grant EP/N023781/1.

## References

- [1] F. Flandoli, *Random Perturbation of PDEs and Fluid Dynamic Models: École d'été de Probabilités de Saint-Flour XL–2010*, vol. 2015. Springer Science & Business Media, 2011.
- [2] D. D. Holm, “Variational principles for stochastic fluid dynamics,” *Proceedings of the Royal Society A: Mathematical, Physical and Engineering Sciences*, vol. 471, no. 2176, 2015.
- [3] T. M. Bendall and C. J. Cotter, “Statistical properties of an enstrophy conserving finite element discretisation for the stochastic quasi-geostrophic equation,” *Geophysical & Astrophysical Fluid Dynamics*, pp. 1–14, 2018.
- [4] C. Cotter, D. Crisan, D. D. Holm, W. Pan, and I. Shevchenko, “Numerically modeling stochastic Lie transport in fluid dynamics,” *Multiscale Modeling & Simulation*, vol. 17, no. 1, pp. 192–232, 2019.
- [5] R. Camassa and D. D. Holm, “An integrable shallow water equation with peaked solitons,” *Physical Review Letters*, vol. 71, no. 11, p. 1661, 1993.
- [6] D. D. Holm and J. E. Marsden, “Momentum maps and measure-valued solutions (peakons, filaments, and sheets) for the EPDiff equation,” in *The breadth of symplectic and Poisson geometry*, pp. 203–235, Springer, 2005.
- [7] D. Crisan and D. D. Holm, “Wave breaking for the stochastic Camassa–Holm equation,” *Physica D: Nonlinear Phenomena*, vol. 376, pp. 138–143, 2018.
- [8] D. D. Holm and T. M. Tyranowski, “Variational principles for stochastic soliton dynamics,” *Proceedings of the Royal Society A: Mathematical, Physical and Engineering Sciences*, vol. 472, no. 2187, 2016.